European Journal of Soil Science

European Journal of Soil Science, September 2017, **68**, 605–620 doi: 10.1111/ejss.12449

Nested sampling and spatial analysis for reconnaissance investigations of soil: an example from agricultural land near mine tailings in Zambia

R. M. Lark[a], E. M. Hamilton[a], B. Kaninga[b,c], K. K. Maseka[d], M. Mutondo[d], G. M. Sakala[b,c] & M. J. Watts[a]

[a]*Centre for Environmental Geochemistry, British Geological Survey, Keyworth, Nottingham, NG12 5GG, UK,* [b]*Zambia Agriculture Research Institute, Mount Makulu, Central Research Station, Lusaka, Zambia,* [c]*University of Zambia, Great East Road Campus, Lusaka, Zambia, and* [d]*Copperbelt University, Jambo Drive, Riverside, Kitwe, Zambia*

Summary

A reconnaissance survey was undertaken on soil near mine tailings to investigate variation in the content of copper, chromium and uranium. A nested sampling design was used. The data showed significant relations between the content of copper and uranium in the soil and its organic matter content, and a significant spatial trend in uranium content with distance from the tailings. Soil pH was not significantly related to any of the metals. The variance components associated with different scales of the sample design had large confidence intervals, but it was possible to show that the random variation was spatially dependent for all spatial models, whether for variation around a constant mean, or with a mean given by a linear effect of organic matter or distance to the tailings. For copper, we showed that a fractal or multifractal random model, with equal variance components for scales in a logarithmic progression, could be rejected for the model of variation around the fixed mean. The inclusion of organic matter as an explanatory factor meant that the fractal model could no longer be rejected, suggesting that the effect of organic matter results in spatial variation that is not scale invariant. It was shown, taking uranium as a case study, that further spatially nested sampling to estimate scale-dependent variance components, or to test a non-fractal model with adequate power, would require in the order of 200–250 samples in total.

Highlights

- Sampling was undertaken to investigate spatial variation of metal content in soil near mine tailings.
- Chromium and uranium were related to soil organic matter content; uranium showed a spatial trend.
- Spatial variation was scale dependent, variation of copper was not scale-invariant.
- Characterizing random spatial variation requires substantial sample effort.

Introduction

Reconnaissance investigations of the soil may be undertaken prior to detailed sampling for tasks such as spatial mapping, or the design of field experiments in which soil variation may be an important source of the residual variance of the observed response. Appropriate reconnaissance sampling supports decisions on the design of subsequent sampling or experiments, and can enable initial testing of hypotheses about the sources of variation in soil properties of interest. In this paper we present a case study in which spatially nested sampling (Youden & Mehlich, 1937) was used for reconnaissance survey of soil prior to the establishment of more detailed surveys and plot experiments on land immediately adjacent to mine tailings near Kitwe, the Copperbelt, Zambia.

Mine tailings are a major source of potentially harmful elements (Lottermoser, 2007), and the Copperbelt province of Zambia has a substantial legacy of tailings and other mine wastes from more than 100 years of mining activity (Weissenstein & Sinkala, 2011). The site of the reported study is land immediately adjacent to a large tailings dam. The land is used by a neighbouring village for agricultural production. This paper reports a reconnaissance survey of the soil at this site that was undertaken before more detailed

Correspondence: R. M. Lark. E-mail: mlark@bgs.ac.uk
Received 30 June 2016; revised version accepted 10 May 2017

sampling and the establishment of experimental plots to examine the uptake of potentially harmful elements from the soil there. In this paper we focus on three elements in particular, chromium, copper and uranium. Chromium was of interest because a key objective of the subsequent experimental work was to examine speciation of the element in soil and its uptake by crops, and how this process might be affected by liming, fertilizers and conservation agriculture practices. Copper was examined because it was expected to be a large component of mine wastes; the ores from which the tailings were derived were copper bearing and were processed for extraction of copper. Copper is a potentially harmful element when present in excess, and one possible exposure route to humans and animals is through uptake by food plants (Guo *et al.*, 2010). Finally, we considered the concentrations of uranium in soil. Mining and extraction of copper from ores can concentrate radionuclides in the tailings, giving rise to what is called technically enhanced naturally occurring radioactive material (TENORM). Uranium is often an important constituent of TENORM in copper mine wastes (National Research Council, 1999), including wastes produced from copper mines in the granitic rocks of the Katanga Basin, which includes the Zambian Copperbelt (Katebe *et al.*, 2008).

The aim of the reconnaissance was to provide information about the factors that affect the spatial variation of concentrations of chromium, copper and uranium across the site. In particular, we wanted to find evidence of a trend in the concentration of the elements with distance from the mine tailings. This would give insight into how the material might disperse from the tailings on to farmed soil and would enable us to identify sites for experimental plots where large or smaller concentrations might be expected.

We were also interested in whether concentrations of the elements were correlated with basic soil properties. The first property was pH. Mine tailings have large pH values because of the incorporation of lime (Weissenstein & Sinkala, 2011) but farmed soil in the area, other than on dambos (Webster, 1965), is more acidic with pH typically between 4 and 6 (Wilson *et al.*, 1956). The mobility of most metals in soil as free ions is reduced if the pH is increased (McBride, 1994). We might expect, therefore, that soil pH, through its effect on metal mobility and hence the rate of leaching of metals from deposited material, might affect the measured concentrations of the elements of interest.

The second soil property that we considered was the organic matter content. There is evidence that the absorption of copper (Petruzzelli *et al.*, 1978) and uranium (Bednar *et al.*, 2007) by soil depends in part on the organic matter content, and it has also been shown that the organic matter of soil has an effect on the mobility of chromium in experimentally leached columns through adsorption and the reduction of Cr(VI) to Cr(III) (Banks *et al.*, 2006). This suggests that the retention of these metals, and so the observed concentrations, might vary with the organic content of the soil.

With an appropriate sampling design and associated statistical analysis, it is possible to examine how the variation of a soil property depends on spatial scale. This can give practically useful information. If, for example, during reconnaissance the variation of a soil property is found to be dominated by variation at fine spatial scales (e.g. of up to 1 m), then this shows that it should be possible to estimate treatment effects or spatial patterns with greater precision in future experiments or surveys if a local bulking strategy is used with samples formed by aggregating cores from within a small region (e.g. Lark, 2012). The investigation of scale dependence might also give insight into the nature of the underlying variation in the soil. For example, soil variation largely driven by land use is likely to be expressed at different spatial scales from variation caused by bioturbation. For this reason we wished to use a sampling design that would support a spatial analysis. In the short period of time available for reconnaissance we used a spatially nested sampling design (Youden & Mehlich, 1937).

Oliver & Webster (1987) showed how spatially nested sampling designs can be used to investigate soil variation as the reconnaissance phase of survey, and suggested that this might be a useful strategy for examining new areas where there is limited information about scale-dependent variation (Webster & Oliver, 1990). Corstanje *et al.* (2008) used the approach to study soil variation at disparate scales over a relatively large area, and Metcalfe *et al.* (2016) showed how it can be used to investigate scale-dependent variation at within-field scales. However, Papritz *et al.* (2011) showed that the uncertainty associated with estimates of individual variance components from a nested sample may be substantial. This is because the likelihood surface that is explored by numerical optimization to find the estimates of the variance components might not have a well-defined maximum. We computed confidence intervals for individual variance components to examine this uncertainty. We also compared the standard nested model, with different variances at each scale, with an alternative in which the variation over a range of scales shows fractal or multifractal behaviour. We then showed, for the case of soil uranium, the total sample size required to estimate variance components with acceptably narrow confidence intervals or to reject the fractal model in favour of one with more complex scale-dependence with sufficient statistical power. This gives further insight into the suitability of spatially nested sampling for reconnaissance survey in such circumstances.

Methods

Study area

The study area is in the vicinity of tailings at Mopane Mine near Kitwe in the Copperbelt, Zambia (12°47′16.1″S, 28°6′13.2″E). The soil around Kitwe is mapped as the legend unit *Plateau Soils* in the Exploratory Soil Map of Zambia (1:1 000 000) (Ministry of Agriculture, 1991), in legend unit Pu7. This unit comprises soil allocated to the following Soil Units of the FAO classification (FAO-Unesco, 1974): chromi-haplic Acrisol with gleyi-haplic Acrisol and partly skeletal phase dystric Leptosol. The dominant units are well-drained deep to very deep yellowish-red to strong brown friable soil with a fine loamy to clayey texture, showing increased clay content with depth. Figure 1 shows the tailings and the location of the sample sites. Mugala Village is to the north of the tailings, with cultivated land between the buildings of the village and the tailings. Land is also cultivated to the west of the tailings, where

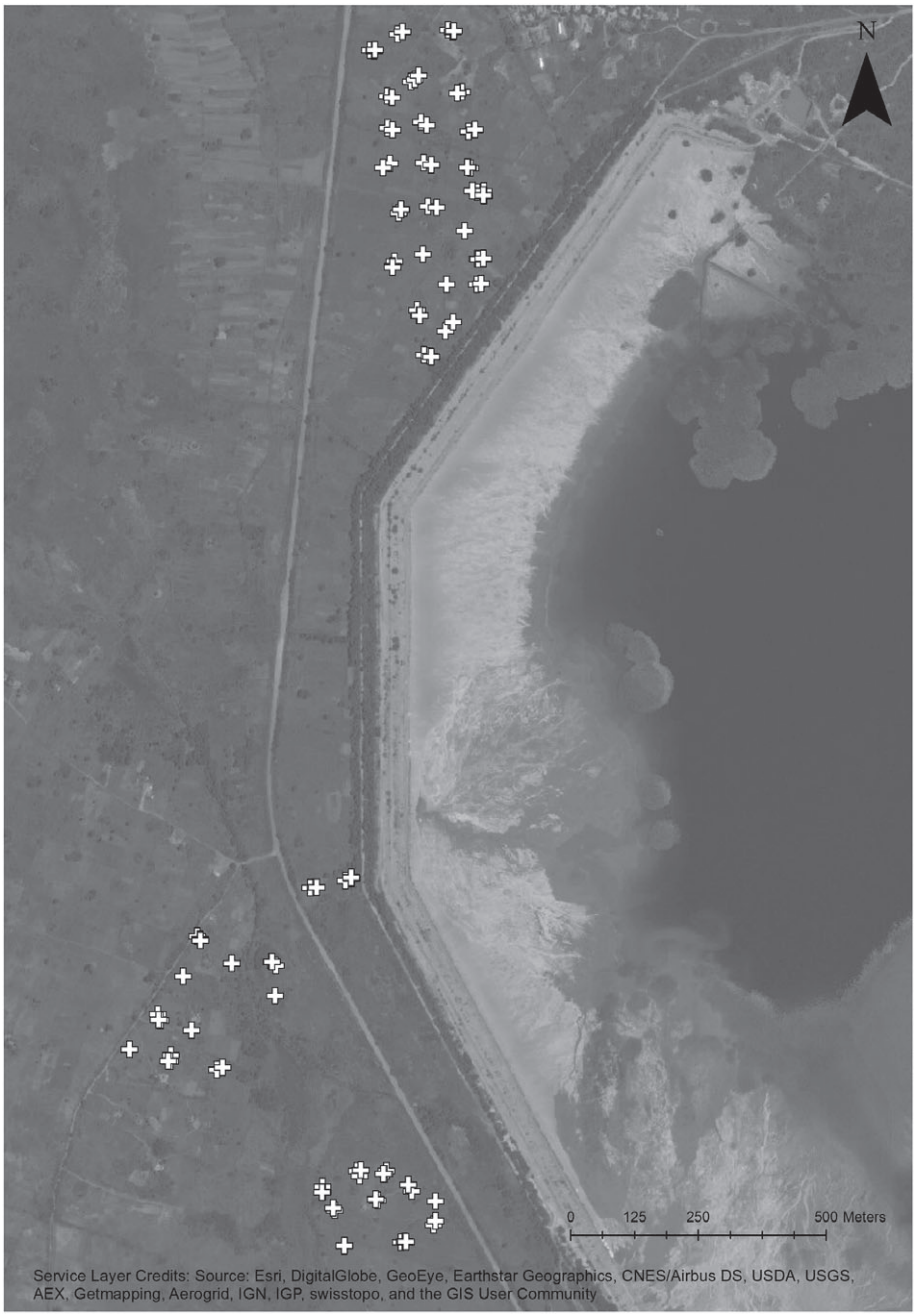

Figure 1 Study site showing sample points (white crosses). Note the tailings dam over much of the east of the image. This image was created with ArcGIS software by Esri. ArcGIS and ArcMap™ are the intellectual property of Esri and are used herein under license. Copyright Esri. All rights reserved.

there is a drainage channel running approximately north to south. Areas of dambo soil occur here, as described by Webster (1965).

Sampling and analysis

The sampling was undertaken according to a nested design. Sample main stations were selected on loose transects with spacing varying between 100 and 200 m and the soil was sampled there. At each main station a substation was selected 100 m from the transect in an approximately normal direction to its orientation. The main station and these initial substations therefore constitute a loose grid. Because their selection was not randomized the associated variance components have a model-based interpretation, that is to say, we assume that the soil variables of interest can be represented as a realization of a random spatial field (Webster, 2000). At each 100-m substation the soil was sampled and then another substation was found 10 m away in a direction selected from a table of random compass bearings. The soil was sampled at the 10-m substation, and then a final substation for the main station was found 1 m away from the 10-m substation in a random direction. This is a 'maximally unbalanced' nested sample design, as first used by Webster & Boag (1992) to examine the distribution of potato cyst

nematodes at within-field scales. Sample locations were recorded with a hand-held GPS. A total of 28 main stations were established, and at one of these two additional samples were collected, giving an additional replicate at the 10 and 1-m scales. There was, therefore, a total of 114 locations, at each of which a soil sample was collected.

At each sample location a composite sample was formed by combining five cores of length 15 cm and diameter 5 cm taken from the vertices and centre of a square of length about 30 cm. The cores were taken with a Dutch auger. At some sites the soil was too fine and dry to form a coherent core, so a sample of comparable volume was taken with a trowel or hoe. The samples were placed in paper sample bags. A few days after collection, the sample volume was reduced by coning and quartering.

Soil from each sample location was analysed in the Inorganic Geochemistry Laboratories of the British Geological Survey. Air-dried soil was sieved to pass 2 mm. The pH of a subsample of the sieved soil was measured with a solid body combined pH electrode in a 0.01 m $CaCl_2$ slurry with a final solid:solution ratio of 1:2.5. A subsample of the remaining sieved soil was milled to < 53 m in an agate ball mill. Loss on ignition (LOI) at 450°C of a 1-g subsample of the milled soil sample was measured. A 10-g subsample of milled soil was mixed thoroughly with 3 g of binder and this mixture was then pressed into a 32-mm diameter pellet using a Herzog press. Total concentrations of a suite of elements were then measured on this pellet by X-ray fluorescence spectrometry (XRFS); wavelength-dispersive XRFS in the case of the elements considered here (Cr, Cu and U). This analysis was carried out at the XRFS laboratory of PANalytical Ltd, Nottingham UK.

Exploratory statistical analyses

Exploratory statistics and plots of the data were examined, and are presented in the results section. In all data with possible contamination we consider the possibility that we have some points that represent point contamination in addition to general diffuse pollution, and soil variation that reflects the natural content of the metals of interest. In statistical analysis of such data, in particular the estimation of variance components or variograms, we do not want such outliers to influence estimates because of their potential disproportionate effects. We computed the median as a robust location statistic for the variables. We also computed the median absolute deviation from the median (MAD), with the MAD procedure for the R platform (R Core Team, 2014). This is a robust measure of variability; the absolute difference of each observation from the median value is computed, and then the median of these differences is found. The value is multiplied by a constant, 1.4826, which makes MAD consistent with the standard deviation of a normal random variable. Any values that were further from the median value by more than $3 \times$ MAD were excluded from analyses as outliers.

Nested linear mixed model (LMM)

Full model: estimation of variance components. The analysis of the data from nested sampling was based on an LMM under which the n observations were treated as realizations of a random variable $Z_{\kappa_1,\kappa_2\ldots,\kappa_m}$ where the subscripts denote the substation at each level of the sampling scheme, in order from the first (main station) to the mth, and:

$$Z_{\kappa_1,\kappa_2\ldots,\kappa_m} = \mathbf{x}^{\mathrm{T}}_{\kappa_1,\kappa_2,\ldots,\kappa_m}\boldsymbol{\tau} + A_{\kappa_1} + B_{\kappa_1,\kappa_2} + \cdots + \varepsilon_{\kappa_1,\kappa_2\ldots,\kappa_m}. \quad (1)$$

Here $\mathbf{x}_{\kappa_1,\kappa_2,\ldots,\kappa_m}$ is a $p \times 1$ vector of fixed effects. In the simplest case there is a single fixed effect that is a constant mean, so $p = 1$, $\mathbf{x}$ is a singleton equal to 1 and the 1×1 vector $\boldsymbol{\tau}$ contains the mean of the variable (fixed-effect coefficient). The alternative model, considered in this study, allowed the mean to vary as a linear function of some secondary variable, so $p = 2$ and $\mathbf{x}$ was a 2×1 vector, with value 1 in the first row and value of the secondary variable in the second row. In this model the first value in $\boldsymbol{\tau}$ is a constant and the second value is a linear regression coefficient for the secondary variable.

The remaining terms on the right-hand side of Equation (1) are random effects, all with mean zero. The variable A_{κ_1} is the effect of the κ_1th main station (i.e. the difference between the mean for that main station and the expected value under the particular fixed effects model). Likewise, B_{κ_1,κ_2} is the effect of the κ_2th substation at level 2 within the κ_1th main station, and so on. In this case it is the difference seen over a 100-m increment at that main station; therefore, the levels of the hierarchical sampling scheme correspond to spatial scales. The variances of the random variables A_{κ_1}, B_{κ_1,κ_2}, $\ldots$, $\varepsilon_{\kappa_1,\kappa_2\ldots,\kappa_m}$ are denoted by $= \{\sigma_1^2, \sigma_2^2, \ldots, \sigma_m^2\}$. We must estimate the variances, and because the sampling design is unbalanced, this is best done by residual maximum likelihood (REML) as described by Webster *et al.* (2006). The analysis entails the assumption that the vector of observations $\mathbf{z}$ is a random variate with distribution:

$$\mathbf{z} \sim \mathcal{N}\{\mathbf{X}^{\mathrm{T}}\boldsymbol{\tau}, \mathbf{V}\}, \quad (2)$$

where $\mathbf{X}$ is an $n \times p$ overall design matrix for the fixed effects, of which the vectors $\mathbf{x}_{\kappa_1,\kappa_2,\ldots,\kappa_m}$ in Equation (1) are rows.

Consider the kth level of the nested sampling scheme, with n_k substations in total. We define an $n \times n_k$ design matrix $\mathbf{U}_k$ for the random effect at this level. The rows of $\mathbf{U}_k$ correspond to the observations, and if a particular observation is in the jth main station at level k then the jth element of the corresponding row of $\mathbf{U}_k$ is 1, and all the others are zero. The overall covariance matrix $\mathbf{V}$ is then obtained by:

$$\mathbf{V} = \sum_{i=1}^{m} \sigma_i^2 \mathbf{U}_i \mathbf{U}_i^{\mathrm{T}}. \quad (3)$$

The natural logarithm of the residual likelihood is given by:

$$\ell_{\mathrm{R}}(\ |\mathbf{z}) = -\frac{1}{2}\left(\ln|\mathbf{V}| + \ln\left|\mathbf{X}^{\mathrm{T}}\mathbf{V}^{-1}\mathbf{X}\right| + \mathbf{z}^{\mathrm{T}}\mathbf{P}\mathbf{z}\right), \quad (4)$$

where **P** is:

$$\mathbf{P} = \mathbf{V}^{-1} - \mathbf{V}^{-1}\mathbf{X}\left(\mathbf{X}^{\mathrm{T}}\mathbf{V}^{-1}\mathbf{X}\right)^{-1}\mathbf{X}^{\mathrm{T}}\mathbf{V}^{-1}. \quad (5)$$

With the data known (**z**) and the design matrices for the fixed and random effects specified (**X** and $\mathbf{U}_i$, $i = 1, 2, \ldots, m$, respectively), $\ell_{\mathrm{R}}(\ |\mathbf{z})$ depends only on the variance components, $= \left\{\sigma_1^2, \sigma_2^2, \ldots, \sigma_m^2\right\}$. Values for these that maximize $\ell_{\mathrm{R}}(\ |\mathbf{z})$ can be found numerically. In this study we used the optim procedure in R to find the residual maximum likelihood estimates, with the estimates constrained to be larger than or equal to a very small positive value to avoid negative estimates.

In the setting of the spatially nested design that we have used here, the first variance, σ_1^2 is a between-main station component of variance that has its origin in all sources of variation expressed as scales that contribute to differences between main stations. The additional estimated variance components, $\widehat{\sigma^2}_2, \ldots, \widehat{\sigma^2}_4$, have a spatial interpretation corresponding to 100-, 10- and 1-m within-main station effects. We computed confidence intervals for these estimates following Papritz *et al.* (2011) by evaluating the observed Fisher Information matrix, $\mathbf{J}\left(\log\widehat{\sigma^2}_1, \ldots, \log\widehat{\sigma^2}_4\right)$, where log denotes the natural logarithm. This matrix is the negative Hessian of the residual log likelihood with respect to the log of the variance parameters, that is:

$$\mathbf{J}\left[i,j\right] = -\frac{\partial^2\ell_{\mathrm{R}}(\ |\mathbf{z})}{\partial\log\sigma_i^2\partial\log\sigma_j^2}, \quad (6)$$

which was evaluated at the REML estimates $\widehat{\ } = \left\{\widehat{\sigma^2}_1, \ldots, \widehat{\sigma^2}_4\right\}$. The covariance matrix of the estimated log variance components is given by the inverse of the Fisher Information matrix, $\mathbf{J}^{-1}\left(\log\widehat{\sigma^2}_1, \ldots, \log\widehat{\sigma^2}_4\right)$. The standard error of $\log\widehat{\sigma^2}_i$ is the square-root of the ith element in the main diagonal of $\mathbf{J}^{-1}\left(\log\widehat{\sigma^2}_1, \ldots, \log\widehat{\sigma^2}_4\right)$. Following Pinheiro & Bates (2000) and Papritz *et al.* (2011) we assumed that the $\log\widehat{\sigma^2}_i$ are normally distributed, so the 95% confidence interval was computed from the standard error, and the upper and lower limits were then back-transformed to the original scales of measurement. Note that when an estimated variance component is at the minimum value imposed by the constraint to ensure non-negative values, the confidence interval goes to $[0, \infty]$.

Given initial estimates of the variance components at different scales, more intensive sampling might be planned to obtain more precise estimates, either at the same site or a homologous one. In this study we considered uranium as a case study. We assumed that further sampling would be undertaken to examine the same spatial scales, but with the optimized sampling design for four scales (three within-main station scales) proposed by Lark (2011). For a given sample design, comprising some number of replicates of this within-main station configuration, and for specified values of the variance components, it is possible to evaluate the negative Hessian matrix in Equation (6). It is then possible, by the same assumptions used to compute confidence intervals for the estimates obtained from our data, to compute the expected confidence intervals for the estimates of the same quantities under the proposed sampling scheme. This was done for different numbers of replicates of the eight-site main station of Lark (2011), and assuming the estimated variance components for uranium obtained for the present dataset.

Full model: estimation of fixed effects. The covariance matrix of fixed effects parameters was estimated by:

$$\widehat{\mathbf{C}} = \left(\mathbf{X}^{\mathrm{T}}\mathbf{V}^{-1}\mathbf{X}\right)^{-1}, \quad (7)$$

where the covariance matrix **V** is obtained from the random effects design matrices and estimated variance components as in Equation (3) and **X** is the overall fixed effects design matrix introduced in Equation (2). In the case of models with a secondary variable treated as a fixed effect, one may test the null hypothesis that the coefficient τ_1 is zero by computing the Wald statistic:

$$W = \frac{\tau_1^2}{\sigma_{\tau_1}^2}, \quad (8)$$

where $\sigma_{\tau_1}^2$ is the variance of the coefficient, in the second element of the main diagonal of **C**. Under the null hypothesis, the Wald statistic is distributed as χ^2 with 1° of freedom.

Alternative variance models. After estimating the full nested model, we considered a simpler model in which the random effects are represented by a single independently and identically distributed (iid) normal random variable. Under this model there is no spatial dependence in the variable of interest. This model was fitted to assess the strength of evidence for spatial dependence by treating it as a null model to be compared with the full model, described above, in which there is a separate variance component estimated for each scale of the sampling design. The comparison was carried out by computation of the log-likelihood ratio statistic L:

$$L = 2\left(\ell_{\mathrm{F}} - \ell_{\mathrm{N}}\right), \quad (9)$$

where ℓ_{F} and ℓ_{N} are, respectively, the maximized log residual likelihood for the full model and the null model. The two models are nested in the sense that the null model can be regarded as a special case of the full model with one or more parameters set to some fixed value. In the standard case the statistic L is asymptotically distributed as χ_p^2, where p is the number of free parameters in the full model that are fixed in the null. The standard case (Stram & Lee, 1994), however, holds only when the parameters fixed in the null model are not fixed at boundary values for the parameter space. For the comparison of the full nested model with the iid null model this condition is not met because the additional parameters are fixed at zero in the null model, which is at the boundary of the parameter space. For this reason the distribution of L under the null model was approximated by a parametric bootstrap simulation. Data were simulated from an iid model, and the maximized residual likelihood was found for each model and L was computed. This was repeated

Table 1 Summary statistics for all variables

Variable	Mean	Standard deviation	Median	MAD[a]	Minimum[b]	Maximum	Skewness	Kurtosis
pH	5.55	0.85	5.48	0.82	3.82	7.32	0.43	−0.60
LOI / %	6.44	1.64	6.00	1.24	2.36	10.80	0.45	0.22
Cr / mg kg^{-1}	70.9	17.5	70.8	12.3	37.2	203.3	3.70	26.59
Cr[c] / mg kg^{-1}	69.7	12.3	70.7	12.0	37.2	107.3	−0.02	0.23
Cu / mg kg^{-1}	1018.8	457.7	972.9	431.8	112.9	2852.0	0.96	2.07
Cu[c] / mg kg^{-1}	988.2	398.9	967.3	421.1	112.9	2102.6	0.26	−0.28
U / mg kg^{-1}	4.04	0.77	3.95	0.82	2.5	8.0	1.09	4.35
U[c] / mg kg^{-1}	4.01	0.68	3.9	0.74	2.5	5.4	0.03	−0.77

[a]Median absolute deviation from the median.
[b]The detection limits for Cr, Cu and U are 3, 1.3 and 0.5 mg kg^{-1}, respectively.
[c]Variable edited by removal of outliers as described in text.
LOI, loss on ignition; MAD, median absolute deviation from the median.

for $M = 10\,000$ independent iterations. If M' out of M simulated values of L exceed the observed value $\widehat{L}$, then the approximate P-value is:

$$\widehat{P} = \frac{M'}{M}.$$

One may account for the uncertainty in this approximation by rejecting the null model in the case of observed $\widehat{L}$ at significance level α only if:

$$\left(\alpha - \widehat{P}\right)^2 < \left(2\,\mathrm{se}\left\{\widehat{P}\right\}\right)^2,$$

where se$(\cdot)$ denotes the standard error of the quantity in braces. On this basis it is required that:

$$\left\{\frac{M'}{M} < \alpha\right\} \wedge \left\{\left(\frac{M'}{M} - \alpha\right)^2 > \frac{4M'(M - M')}{M^3}\right\}, \qquad (10)$$

in order to reject the null model at significance level α (Percival & Walden, 2000).

We also considered another variance model, simpler than the full model with four separate variance components, but more complex than the iid model, which has only one non-zero variance component at the finest scale. In the model we considered, the within-main station variance components (i.e. those at 1, 10 and 100 m) are all equal, and a separate variance is estimated for the between-main station effect. This model is of interest because its comparison against the full model allows a test of whether the within-main station variance components are equal. It is also interesting in this case where the within-main station scales are on a logarithmic sequence. Miesch (1975) showed that a plot of the accumulated variance components from fine to coarse scales against the scale length, approximates the variogram of a random variable. Therefore, in the case of logarithmic scale lengths, equal variance components mean that the variogram increases linearly with the logarithm of lag distance. This simple form of variogram is known as the de Wijsian model (Krige, 1981). Chilès & Delfiner (1999) point out that it implies fractal, more generally multifractal, random variation.

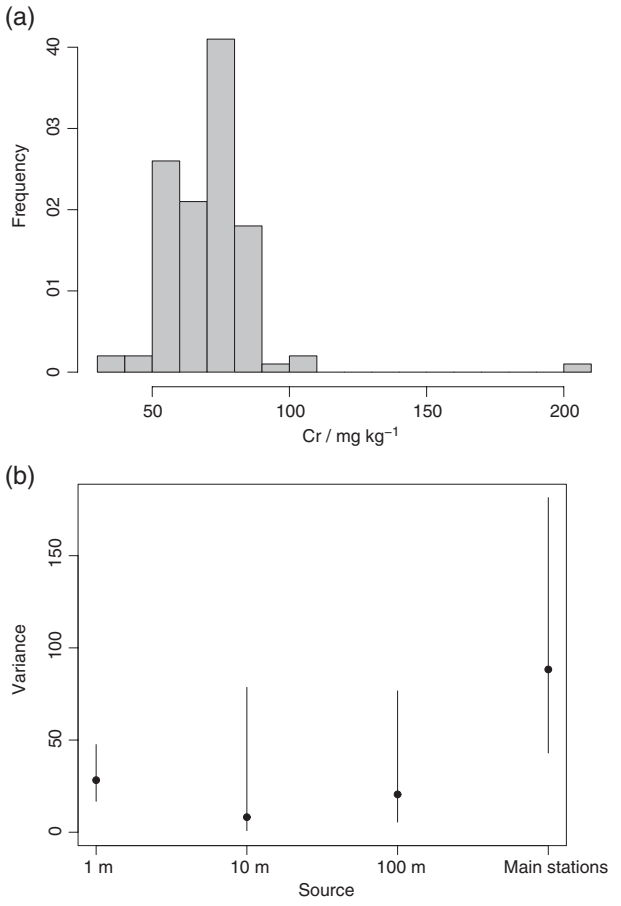

Figure 2 Exploratory plots of data on chromium. The histogram (a) shows the full dataset and (b) shows spatial variance components (after removal of one outlier). Vertical line shows 95% confidence interval for variances.

This form of scale-invariant spatial variability has attracted interest (e.g. Besag & Mondal, 2005; McCullagh & Clifford, 2006). In particular, Lovejoy & Schertzer (2007) suggest that multifractal scaling behaviour, commonly identified in atmospheric phenomena, can be identified in terrestrial processes. They argue against what they call

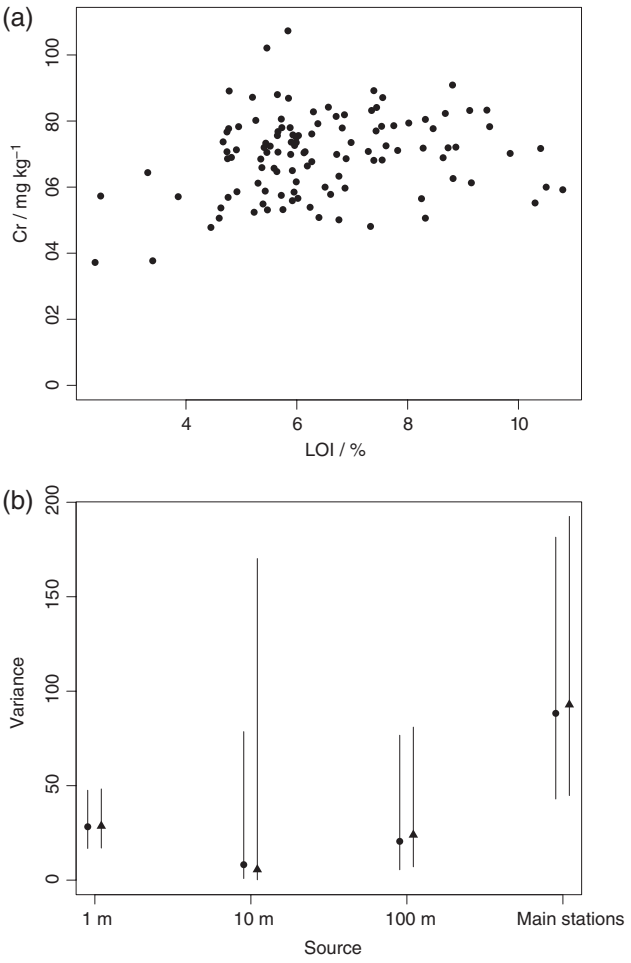

Figure 3 (a) Plot of chromium concentration against loss on ignition (LOI) and (b) variance components of chromium with fixed effects a constant mean (●) or LOI (▲). Vertical line shows 95% confidence interval for variances.

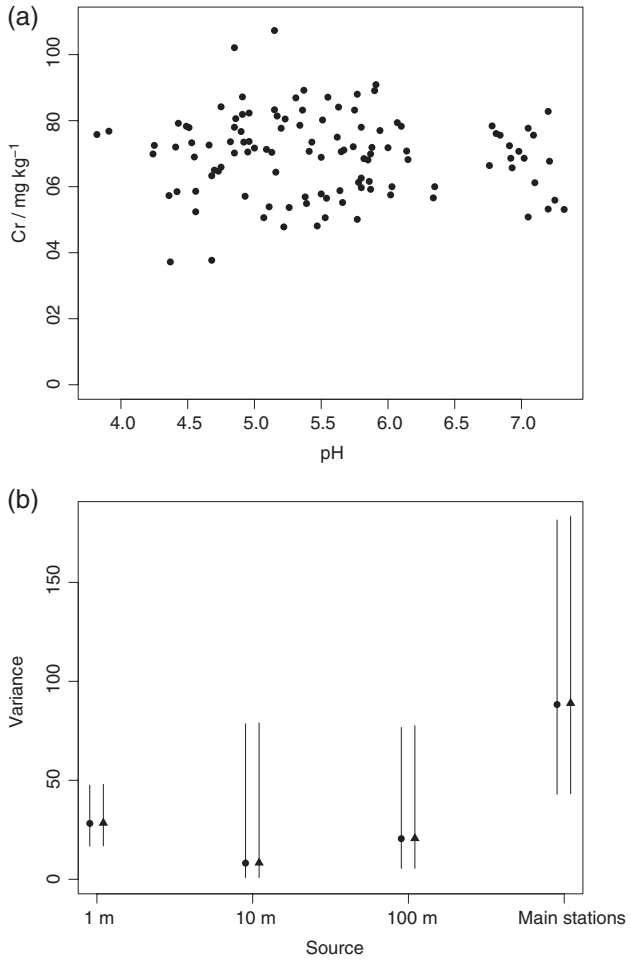

Figure 4 (a) Plot of chromium concentration against pH and (b) variance components of chromium with fixed effects a constant mean (●) or pH (▲). Vertical line shows 95% confidence interval for variances.

a 'phenomenological' interpretation of scale-dependent variation by which different mechanisms are invoked to account for variation at different spatial scales. The phenomenological approach is implicit or explicit in much discussion of spatial and temporal variation of soil (e.g. Hoosbeek & Bryant, 1992; Wagenet, 1998; Vogel & Roth, 2003; Pachepsky & Hill, 2017). For this reason, what we call the fractal variance model, with equal variance components at the within-main station scales, is an interesting alternative to the iid for comparison with the full model. It is more plausible as a null model than the iid because it implies spatial correlation. The comparison with the full model might be illuminating, because evidence against the fractal model (conditional on the selected fixed effects) implies an alternative under which there are distinct, scale-dependent, mechanisms that contribute to soil variation: the phenomenological interpretation of spatial variation. Assessment of the variance components associated with each scale under the full model, and how they change as different covariates are included in the fixed effects, could be a powerful source of insight into the sources of soil variation.

The fractal model can be compared with the full model on the log-likelihood ratio statistic, L. The nested relations of the models can be clarified by a parameterization of the full model in which the variance parameters are a variance component at the finest spatial scale, σ_1^2, and three scaling factors, ξ_2, ξ_3 and ξ_4, such that the variance component at the ith scale is $\sigma_1^2\xi_i$. The fractal model can be seen to be a special case in which $\xi_2 = \xi_3 = 1$. Because this value is not at the boundary of the parameter space, the asymptotic distribution of L for this test under the null model is χ_2^2. This test must be interpreted with caution. Rejection of the fractal null model in favour of the full alternative suggests that the de Wijsian scaling over the within-main station scale range is not plausible, but failure to reject the null model does not necessarily indicate evidence for de Wijsian behaviour, given the uncertainty with which the variance components are estimated.

We considered uranium as a case study for planning further, more intensive, sampling. For this element we simulated a dataset with the estimated variance components and for a sampling design with some specified number of replicates of the eight-site main station

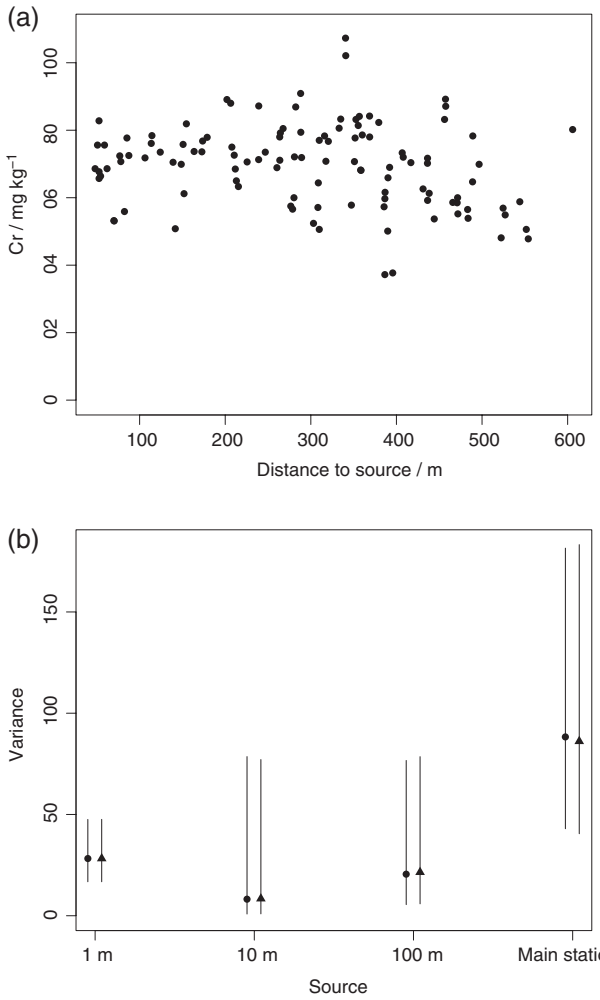

Figure 5 (a) Plot of chromium concentration against distance to tailings and (b) variance components of chromium with fixed effects a constant mean (●) or distance to tailings (▲). Vertical line shows 95% confidence interval for variances.

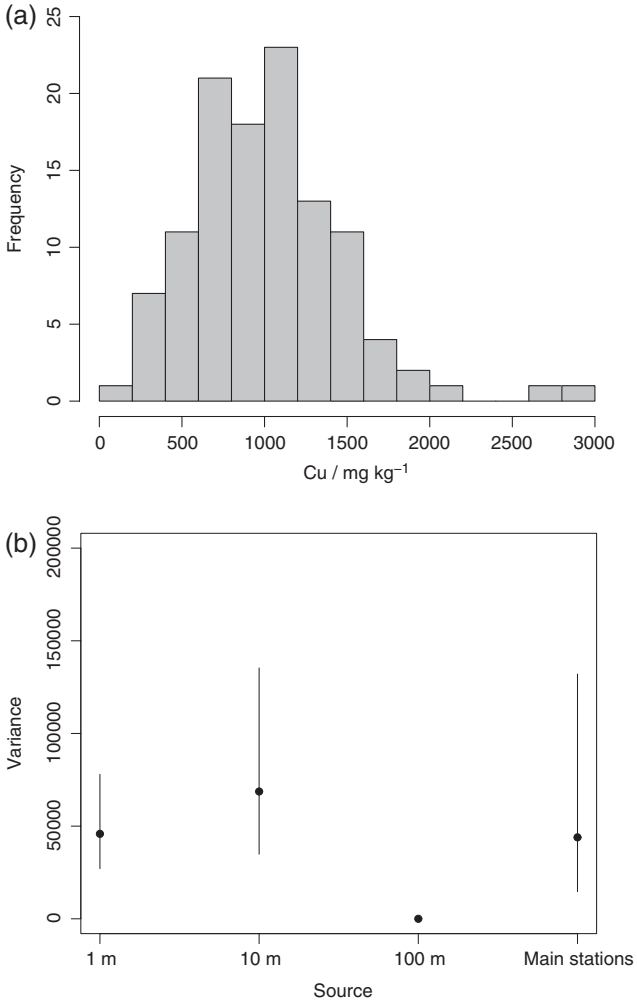

Figure 6 Exploratory plots of data on copper. The histogram (a) shows the full dataset and (b) shows spatial variance components (after removal of one outlier). Vertical line shows 95% confidence interval for variances, except at 100 m where the estimate is zero.

of Lark (2011). We then computed the maximized log-residual likelihoods for the full model and null model, and also the log-likelihood ratio statistic, L. This was repeated 1000 times to give an empirical distribution of L for the specified sample size. Such a distribution was found for sample designs with 6, 12, 18 and 24 replicates of the eight-site main station, giving total sample sizes of 48, 96, 144 and 192. The expected power of the log-likelihood ratio test was evaluated for each sample size as the proportion of simulated values of L that exceed the 95th percentile of the χ^2_2 distribution.

Results

Exploratory analyses

Summary statistics for all variables are listed in Table 1, including values recalculated after exclusion of any outlying values outside the interval (median $-3 \times$ MAD, median $+3 \times$ MAD) where MAD is the median absolute deviation from the median as described above. Note that in all cases the minimum value for total element concentration was larger than the detection limit for the XRFS analysis. Histograms of the data on metal concentrations are shown in Figures 2(a), 6(a) and 10(a) for chromium, copper and uranium, respectively. One outlying datum was removed from each of the datasets on chromium and uranium and two from the data on copper.

Figures 3(a), 7(a) and 11(a) show the data on metal concentrations (after removal of outliers) plotted against loss on ignition; Figures 4(a), 8(a) and 12(a) show them plotted against soil pH and Figures 5(a), 9(a) and 13(a) show them plotted against distance to the tailings.

Nested analyses

Models with the fixed effect a constant mean only. Table 2 shows estimated variance components at each scale for the three metals

Table 2 Nested variance components for the full model where these may vary between scales

Variable	Source				ℓ_{full}	ℓ_{iid}	L^a
	Main station	100 / m	10 / m	1 / m			
Cr / mg kg^{-1}	88.29	20.53	8.17	28.24	−299.80	−339.28	78.96
Cu / mg kg^{-1}	45.76×10^3	0.0	79.58×10^3	35.56×10^3	−708.68	−722.59	27.82
U / mg kg^{-1}	0.235	0.142	0.018	0.070	25.84	−15.22	82.12

[a]Note that critical values of the L statistic determined by parametric bootstrap are: $P < 0.05$, 4.64 ; $P < 0.01$, 7.93 ; $P < 0.001$, 14.63. The largest value of L in 10 000 samples was 19.92.
Also presented are the maximized log-likelihoods for the full model and the independently and identically distributed (iid) null model, and the log-likelihood ratio statistic for the comparison between these.

for the LMM where the only fixed effect is a constant mean. Also shown are the maximized residual log-likelihoods for the full model and the iid null model and the log-likelihood ratio statistics for the comparison between these. Threshold values for the latter from parametric bootstrapping, for rejection of the null model according to the criteria in Equation (10), are in a footnote to the table.

These variance components are plotted in Figures 2(b), 6(b) and 10(b); the vertical bars show the 95% confidence interval for each estimate (where this is not zero). These intervals are generally wide for the scales longer than 1 m, showing the associated uncertainty. The between-main station variance component is the largest for chromium and uranium. For copper the estimated 10-m variance component is largest, the component at 100 m approaches zero (constrained to be positive), but there is substantial overlap between the confidence intervals for the 10-m and between-main station scales.

Table 3 gives the estimated parameters for the fractal model for the LMM with a constant mean, the maximized residual log-likelihoods and log-likelihood ratio statistics for the comparison of the full model against the fractal model.

For all three metals, these results show strong evidence against the iid model (i.e. there is evidence of spatial dependence). For copper, the fractal null model can be rejected; we cannot treat the within-main station variance components as equal. The fractal null model cannot be rejected for uranium and chromium, but the confidence intervals for the variance components are consistent with a range of behaviours, so this cannot be treated as positive evidence *for* a fractal model.

Models with covariates included as fixed effects. Table 4 shows the results from fitting the LMM with linear fixed effects of LOI, pH and distance to tailings, including the Wald statistics for the null hypothesis of no effect and associated P-value. The variance components for the random effects in these models, with their 95% confidence intervals, are plotted in Figures 3(b), 4(b) and 5(b) for chromium, in Figures 7(b), 8(b) and 9(b) for copper and in Figures 11(b), 12(b) and 13(b) for uranium.

These results show a significant relation between LOI and the concentrations of copper and of uranium. There is no evidence of a relation between LOI and chromium content. There is no evidence

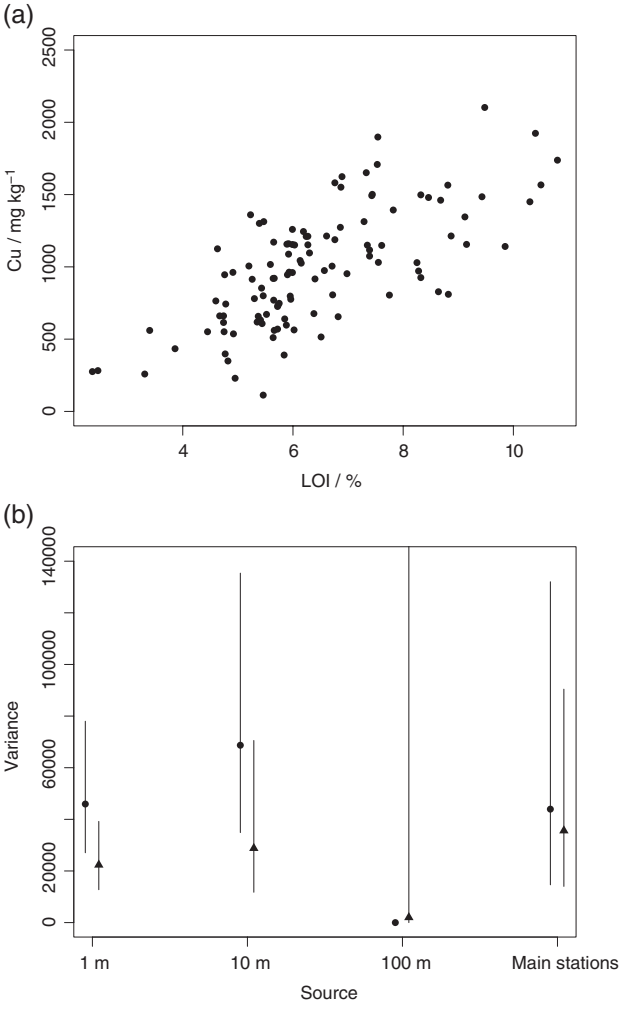

Figure 7 (a) Plot of copper concentration against loss on ignition (LOI) and (b) variance components of copper with fixed effects a constant mean (●) or LOI (▲). Vertical line shows 95% confidence interval for variances.

of a linear trend with distance to the tailings in the concentration of copper or chromium in the soil, but there is a pronounced trend for uranium, which has largest concentrations at short distances from the tailings. There is no evidence of a relation between soil pH and any of the metals considered here.

Table 3 Equal within-main station variance components (fractal)

Variable	Source		ℓ_{fractal}	L^{a}	P
	Main station	Within-main station			
Cr / mg kg^{-1}	85.24 {41.46, 175.24}	21.30 {15.56, 29.16}	−301.0	2.40	0.30
Cu / mg kg^{-1}	20.85×10^{3} {1.98, 219.65}	49.65×10^{3} {36.12, 68.25}	−712.25	7.14	0.03
U / mg kg^{-1}	0.264 {0.129, 0.542}	0.064 {0.047, 0.008}	23.66	4.36	0.11

[a]The likelihood ratio is for a test against the full model reported in Table 2. The *P*-value is the asymptotic value for χ^2_2.
The maximized log likelihood is presented for this model and the log-likelihood ratio statistic for the comparison of the full model against the fractal model and the associated *P*-value.

Table 4 Models for metal concentrations with loss on ignition (LOI), pH or distance to tailings (DtT) as covariates. For each predictor we present the intercept (τ_0) and the fixed effect coefficient (τ_1), the variance of the latter ($\widehat{\sigma^2}_{\tau_1}$) and the Wald statistic and associated *P*-value for the null hypothesis that the fixed effect coefficient is zero. The log-likelihood for the fitted model is also presented

Variable	Predictor	τ_0	τ_1	$\widehat{\sigma^2}_{\tau_1}$	Wald $_{\tau_1}$	P	ℓ_{full}
Cr / mg kg^{-1}	LOI / %	73.5	−0.564	0.422	0.75	0.38	−299.94
	pH	71.0	−0.220	2.05	0.02	0.88	−299.42
	DtT[a] / m	72.3	−0.009	0.2×10^{-3}	0.42	0.52	−303.92
Cu / mg kg^{-1}	LOI / %	−321.2	204.7	378.9	112.7	< 0.001	−667.47
	pH	551.7	82.6	2638.5	2.59	0.11	−703.51
	DtT[a] / m	960.8	0.16	0.14	0.17	0.68	−709.59
U / mg kg^{-1}	LOI / %	3.16	0.132	0.001	15.1	< 0.001	28.72
	pH	3.78	0.045	0.006	0.35	0.55	23.43
	DtT[a] / m	4.67	−2.15	0.4×10^{-6}	12.5	< 0.001	23.05

[a]Distance to tailings.

Table 5 shows the maximized residual log-likelihoods for the alternative random effects models for the three cases where a significant effect of one of the covariates was identified with the full random effects model. Also given are the log-likelihood ratio statistics to test the full random effects model (four separate variance components) against the null and the fractal alternative models, respectively, and the corresponding *P*-values for the log-likelihood ratio test of the full model against the fractal null model.

In all cases the iid null model can be rejected. The fractal null model can be rejected for the LMM for uranium where there is a fixed effect of distance to tailings. In the other two cases it cannot, but, as for the previous models, given the wide confidence intervals for the individual variance components it is not safe to draw any inference from the failure to reject the null model.

Although we can reject the fractal null model for copper with a constant fixed effect, when LOI is included as a covariate the fractal model cannot be rejected. Note that the largest difference in variance components between the models with and without a fixed effect of LOI (Figure 7(b)) is at 10 m, but the confidence intervals of the estimates are wide.

The estimated variance components for uranium are changed little by including LOI as a covariate, although this does have a significant effect. Including distance to tailings has the largest effect on the between-main station variance component for uranium (although note, again, the wide confidence interval). However, we can reject the fractal null model in this latter case, which appears to result from an increase in the estimated variance at 100 m. The distance to tailings effect therefore seems to account primarily for between-main station variation, as would be expected, but somewhat inflates the error in the model at the 100-m scale. Presumably this is because the trend model, dominated by the effects seen between main stations, introduces variations into the fitted values that are notable at the 100-m scale but are not consistent with the variations seen at that scale within the main stations.

Implications for further sampling of uranium. Figure 14 shows the width of the confidence intervals (95%) for U with a constant mean as the fixed effect and different sample sizes with the main station design of Lark (2011). The confidence intervals for the 1-m scale and the between-main station effects, and for the 10-m scale and the between-main station effects do not overlap with a total of 96 samples (nine main stations) or more. With 144 samples (18 main stations) the intervals for the 10 and 100-m scales do not overlap. With 240 samples (30 main stations) the intervals for the 1 and 10-m scales do not overlap. The intervals for the 100-m and between-main station scales overlap for all sample sizes considered. On this basis one might identify a total sample size of near to 240 as required to obtain distinct estimates of the variance components for U at the scales of interest.

Figure 15 shows the power to reject the fractal null model with different numbers of replicates of the main-station design of Lark (2011). With a total of 144 samples (18 main stations) the power

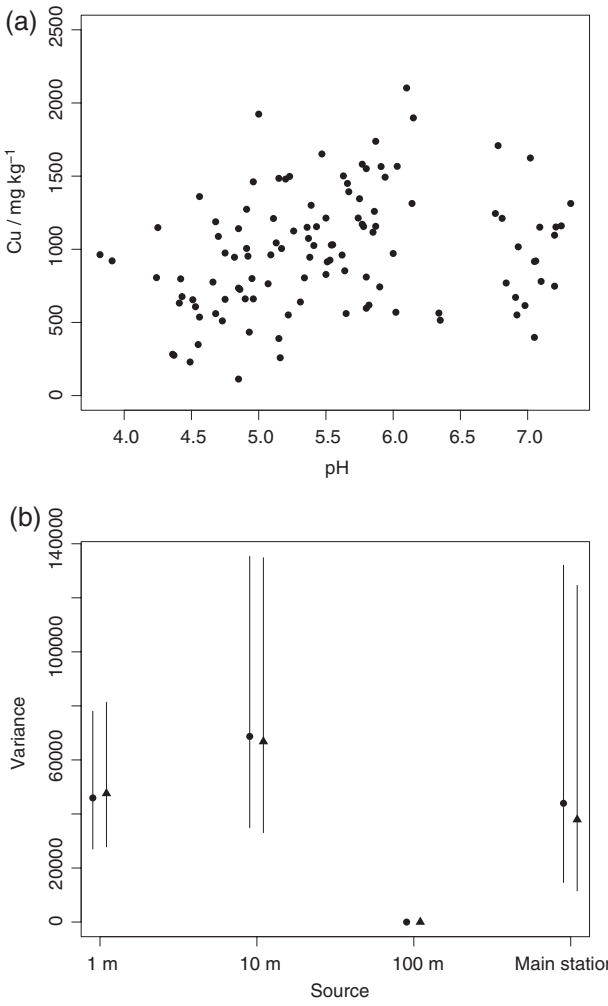

Figure 8 (a) Plot of copper concentration against pH and (b) variance components of copper with fixed effects a constant mean (●) or pH (▲). Vertical line shows 95% confidence interval for variances.

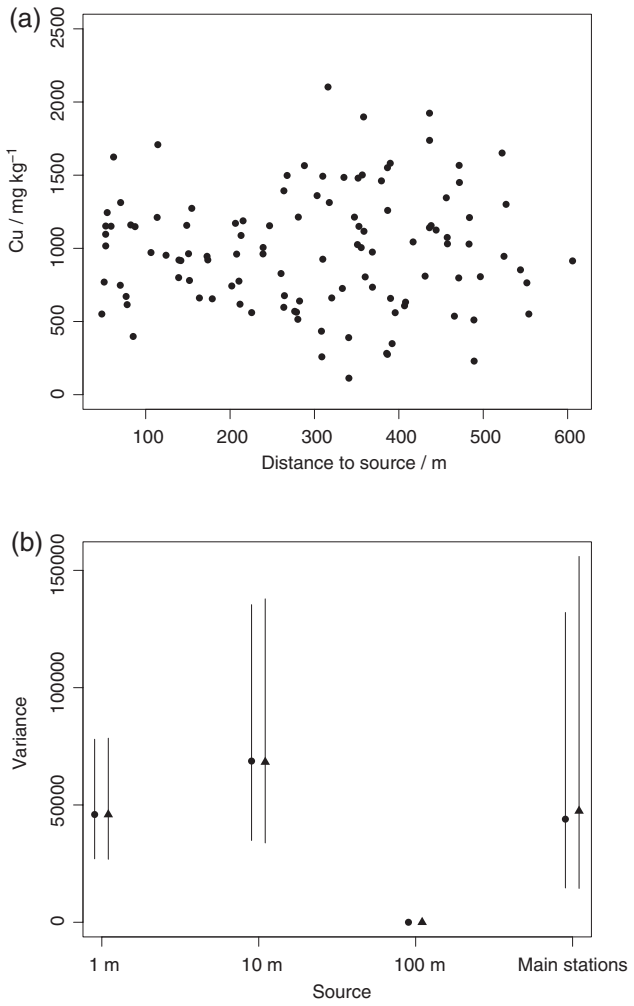

Figure 9 (a) Plot of copper concentration against distance to tailings and (b) variance components of copper with fixed effects a constant mean (●) or distance to tailings (▲). Vertical line shows 95% confidence interval for variances.

is less than 0.8, but it exceeds this threshold with 192 samples (24 main stations). This indicates the sampling effort needed to detect differences between the variance components at within-main station scales if the size of these is indicated by the estimates obtained here.

Discussion

The effects of LOI on the copper and uranium content of the soil are interesting; they suggest that these metals are retained by the organic matter in the soil. As noted in the introduction, there is reason to expect a similar effect for chromium, partly because of adsorption and also reduction to less mobile forms. The further work planned on speciation of chromium in the soil of this region might shed light on why there is no evidence for an effect of organic matter content. Conservation agriculture practices can be expected to increase the organic status of the soil. Any changes in soil management that affect turnover of soil carbon might have an effect on copper availability, for example if dissolved organic matter in the soil solution was increased (Temminghoff *et al.*, 1998). These results suggest that a possible effect would be increased retention of potentially harmful elements in the soil, although if the interaction with soil organic carbon reduces availability to plant roots then this might reduce the risk of transfer to humans through consumption of food. Further work is planned, both in field and glasshouse trials, to examine uptake of metals by crops in soil from this site. These results suggest that it would be worth examining the effects of soil organic matter on bioavailability.

A spatial trend with distance to tailings was seen for uranium only. This might be because of differences in the metal content of contrasting size fractions of the tailings material, which differ in their susceptibility to dispersal by wind. Other metals may be dispersed from tailings by run-off, by use of water from tailing streams for irrigation or by more diffuse deposition. The marked trend in uranium concentrations is important to consider

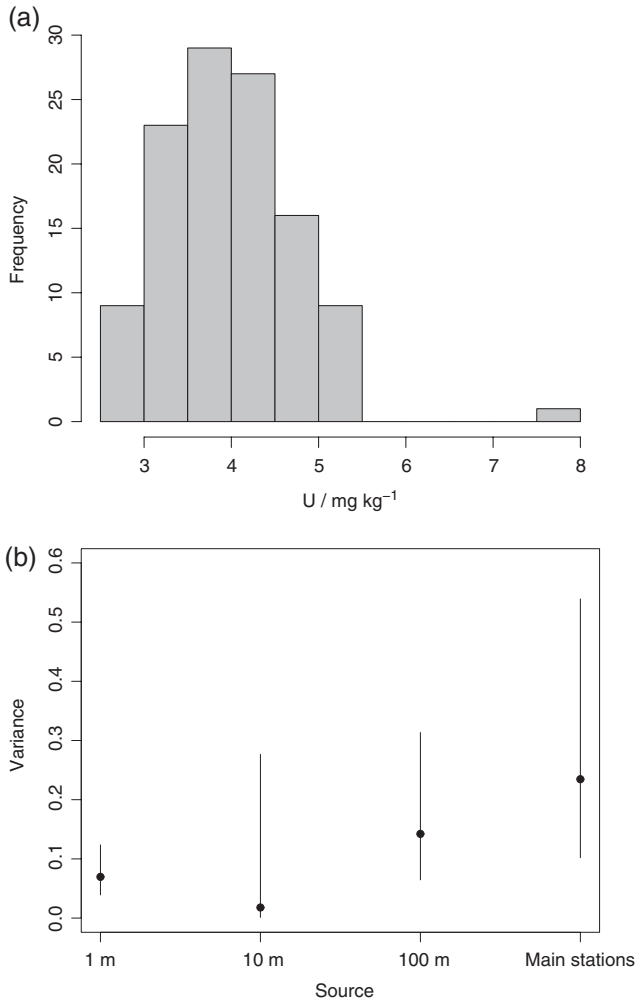

Figure 10 Exploratory plots of data on uranium. The histogram (a) shows the full dataset and (b) shows spatial variance components (after removal of one outlier). ● Vertical line shows 95% confidence interval for variances.

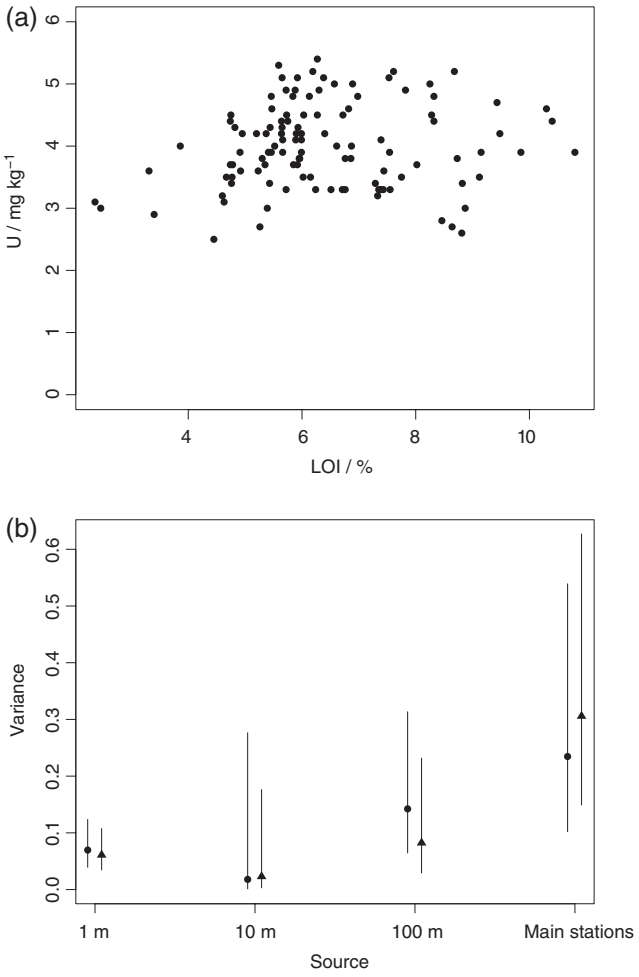

Figure 11 (a) Plot of uranium concentration against loss on ignition (LOI) and (b) variance components of uranium with fixed effects a constant mean (●) or LOI (▲). Vertical line shows 95% confidence interval for variances.

when evaluating potential risks from TENORM associated with tailings dams.

The partition of variation by a linear mixed model into fixed and random effects is not unique, but is a decision made by the analyst. The analyst does not have complete freedom in this regard; for example, it might be necessary to include coordinates in the fixed effects to account for a spatial trend that is not compatible with the assumption of a zero mean in the random effects. Nevertheless, it might be informative to compare properties of the random effects in two models for the same data that differ with respect to the fixed effects. For example, if the inclusion of a particular term in the fixed effects leads to a marked change in the distribution of the random variation between scales then this might indicate the spatial scale at which that term affects the variation of the dependent variable. An example is provided by comparison of the random effects in the models for copper with a constant fixed effect and with LOI as a fixed effect. The fractal model was rejected in the former case, but was accepted when LOI was included as a fixed effect. This suggests that the effect of soil organic carbon induces variation in soil copper content that is not consistent with simple fractal or multifractal scaling. To complement this analysis with evidence that a fractal model is reasonable in other circumstances would require more intensive sampling to increase the power to reject the fractal null model under appropriate circumstances. This is discussed below for the case of uranium.

The inclusion of distance to tailings as a fixed effect in the model for U is shown to make the within-main station variances less uniform (fractal model retained with constant fixed effect, rejected when distance is included). The variance component estimates, although uncertain, suggest that this effect is a result of an increase in the 100-m scale variance. Overall, the distance effect is significant, and it accounts for variation at between-main station scales. However, the slight inflation of the variance at the longest within-main station scale is interesting, suggesting that other factors dominate variation at this scale. This shows the importance of examining scale dependence of the random variation in any linear model to understand better its 'lack of fit'.

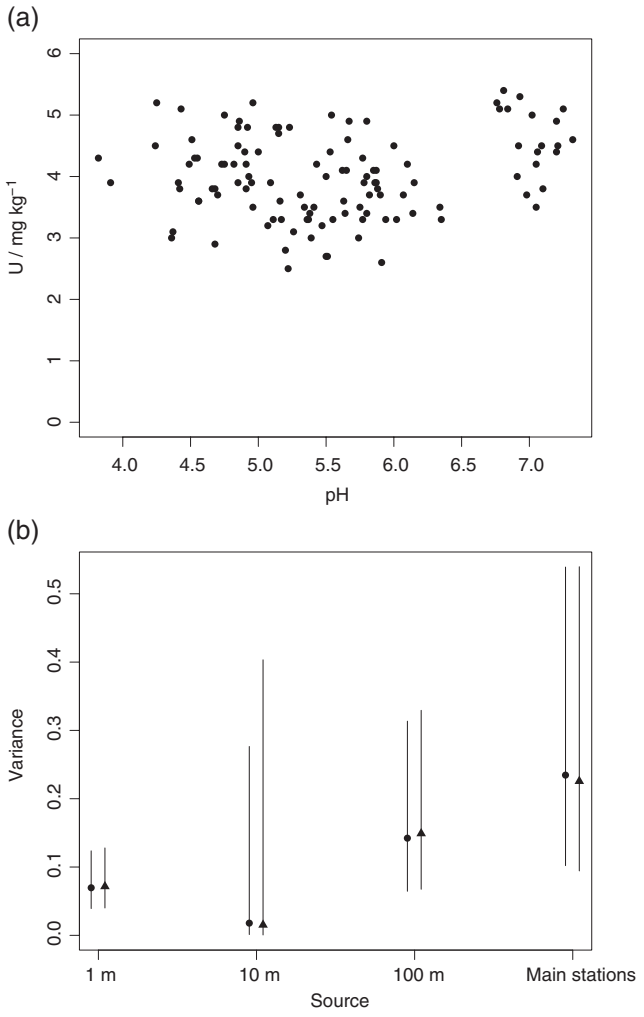

Figure 12 (a) Plot of uranium concentration against pH and (b) variance components of uranium with fixed effects a constant mean (●) or pH (▲). Vertical line shows 95% confidence interval for variances.

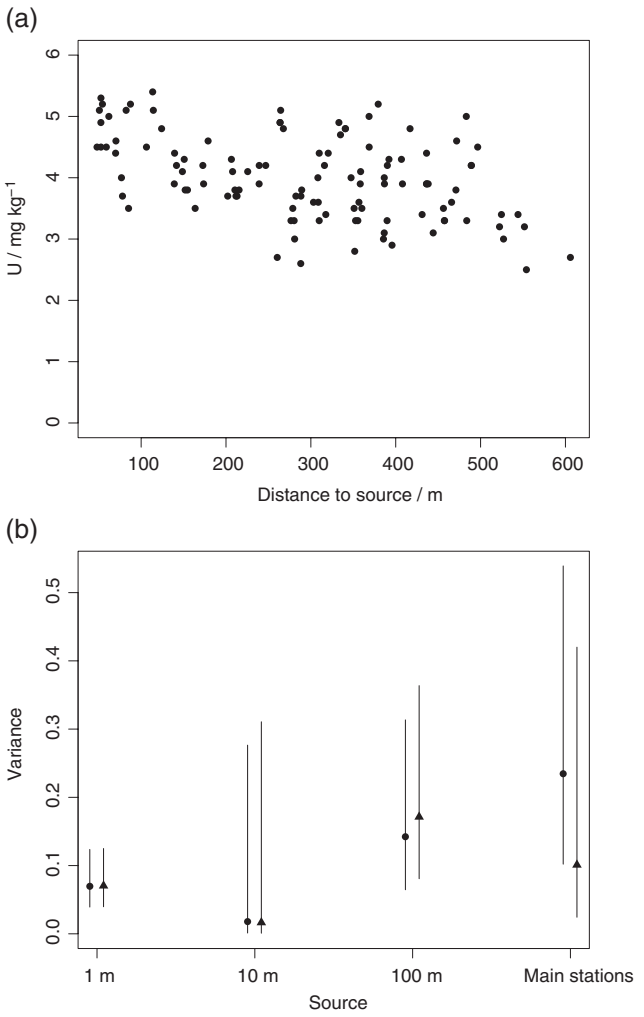

Figure 13 (a) Plot of uranium concentration against distance to tailings and (b) variance components of uranium with fixed effects a constant mean (●) or distance to tailings (▲). Vertical line shows 95% confidence interval for variances.

The conclusions about sampling requirements for further work on uranium show that substantial sample effort is needed to make reliable estimates and to support inferences with sufficient power. Many studies that use nested sampling do not approach the degree of replication that these results show is necessary and, as first raised by Papritz *et al.* (2011), it is necessary to understand better the sampling requirements for nested sampling to examine scale-dependent variation. If we wish to understand scale-dependent variation over multiple scales some form of nested sampling is necessary, but adequate sampling effort is also required. For uranium, we require 200–250 samples to estimate variance

Table 5 Likelihood ratio tests to compare alternative variance models when the fixed effects include a predictor judged to be significant

		Negative log-likelihood for alternative variance models						
Variable	Predictor	ℓ_{full}	ℓ_{fractal}	ℓ_{iid}	$L_{\text{full vs fractal}}$	$P_{\text{full vs fractal}}$	$L_{\text{full vs iid}}$	$P_{\text{full vs iid}}$
Cu / mg kg^{-1}	LOI	−667.47	−668.19	−683.19	1.54	0.46	31.44	< 0.001
U / mg kg^{-1}	LOI	28.72	27.99	−17.57	1.46	0.48	92.58	< 0.001
U / mg kg^{-1}	DtT	23.05	19.95	−9.81	6.20	0.045	65.72	< 0.001

LOI, loss on ignition; DtT, distance to tailings.

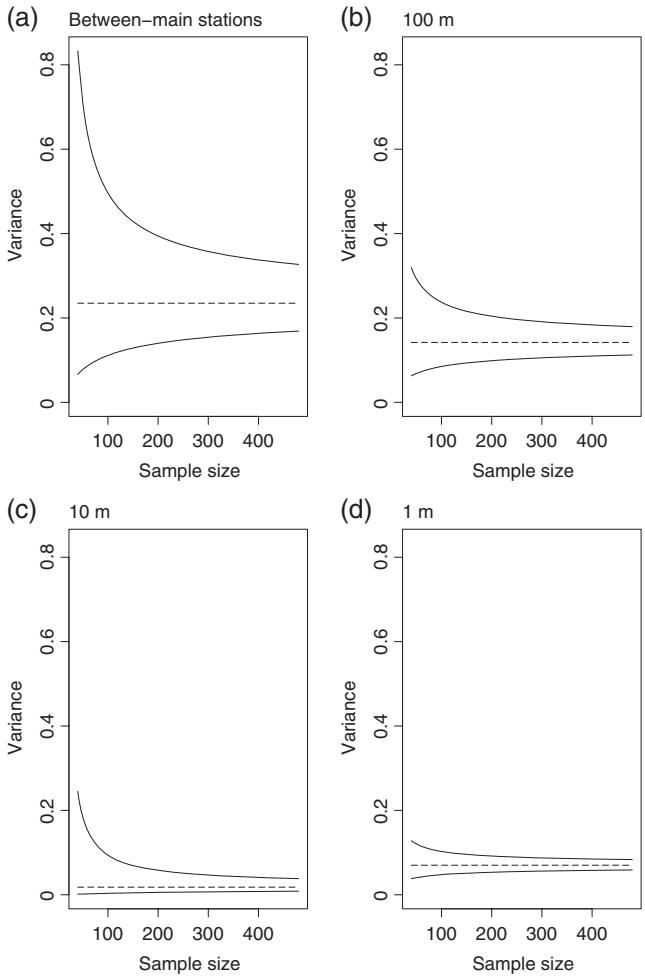

Figure 14 Confidence intervals (95%) for estimated variance components of U at each scale of the design, computed for the main station design of Lark (2011) with different numbers of replicates, and assuming the values presented in Table 2. The parts show confidence intervals of the variance components for (a) between-main station effect, (b) 100-m scale effect, (c) 10-m scale effect and (d) 1-m scale effect.

components precisely, and to reject the fractal null model with sufficient power. This sample size is large for reconnaissance purposes. When a key objective of reconnaissance is to understand scale dependence of variation over disparate spatial scales, then the requirement for substantial sampling effort is unavoidable. One way to mitigate this problem, particularly with respect to analytical laboratory costs, might be to use rapid in-field measurement (Hartemink & Minasny, 2014), to obtain more observations than conventional field sampling and laboratory analysis.

Conclusions

This reconnaissance survey identified key factors that affect the spatial variation of the metals of interest in soil used for agriculture on a site next to mine tailings. Copper content of the soil was significantly correlated with the organic matter content, suggesting

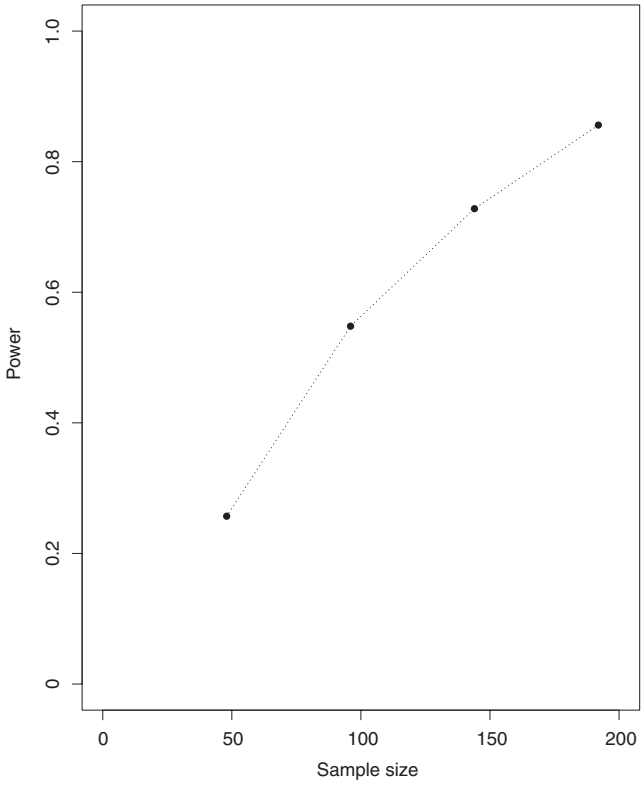

Figure 15 Power to reject the fractal null model in favour of the full model for U (fixed effect a constant mean) computed by simulation assuming the effects of interest are the estimated variance components, and the sample design is that of Lark (2011).

that the adsorption of copper by the organic fraction of the soil might increase its retention by contaminated soil. This provides important background information for the further work planned at the site. Specifically, it suggests that hypotheses should be tested about the effect of soil organic matter on the content and availability of copper to crop plants, and the possibility that uptake by crops is a pathway for soil to human transfer of a potentially harmful element. Given the interest in agricultural practices to increase the organic content of soil, this is an important question. The same issue is raised for uranium in this soil, but there is no evidence that the content of chromium is affected by organic carbon. Of the three metals examined, uranium was the only one for which there was a clear spatial trend (decreasing content) with increasing distance from the mine tailings.

The uncertainties associated with the variance components at different spatial scales was considerable. However, it was possible to draw some conclusions about the spatial variation of the metals by statistical comparison of contrasting variance models. In all cases the random variation (whether in a model with a constant mean as the only fixed effect, or an effect of organic matter or distance to tailings) showed spatial dependence. In the case of copper there was evidence (with a constant mean the only fixed effect) that one could reject a fractal model in which the variance components at 1, 10 and 100 m were equal in favour of a model with distinct

scale-dependent effects. Introducing soil organic matter content as a fixed effect changed this conclusion; the fractal model could not be rejected. This suggests that the effects of organic matter on copper content represent a distinct, scale-dependent source of variation in soil copper content, which therefore does not show simple scale-invariant behaviour.

The study on sampling requirements for uranium indicated that larger samples would be required to obtain narrow confidence intervals for the variance components (around 240) and to allow rejection of the fractal model in favour of one with distinct variance components equal to the estimates from the reconnaissance (approaching 200 samples). This suggests that sampling at multiple scales requires more effort than is generally available for reconnaissance survey as such. Quicker and cheaper measurement, perhaps with in-field technology, should be explored.

Acknowledgements

This paper is published with permission of the Executive Director of the British Geological Survey (NERC). Field and laboratory work for this project was funded by The Centre for Environmental Geochemistry and BGS Global. Author contributions were supported by the UK Department for International Development (DFID) through a Royal Society and DFID Africa Capacity Building Initiative (ACBI) Programme Grant, Award AQ140000. We acknowledge the assistance of staff from ZARI and students at Copperbelt University for help with field sampling.

References

Banks, M.K., Schwab, A.P. & Henderson, C. 2006. Leaching and reduction of chromium in soil as affected by soil organic content and plants. *Chemosphere*, **62**, 255–264.

Bednar, A.J., Medina, V.F., Ulmer-Scholle, D.S., Frey, B.A., Johnson, B.L., Brostoff, W.N. *et al.* 2007. Effects of organic matter on the distribution of uranium in soil and plant matrices. *Chemosphere*, **70**, 237–247.

Besag, J. & Mondal, D. 2005. First-order intrinsic autoregressions and the de Wijs process. *Biometrika*, **92**, 909–920.

Chilès, J.-P. & Delfiner, P. 1999. *Geostatistics: Modeling Spatial Uncertainty*. Wiley, New York.

Corstanje, R., Pawlett, M., Read, R., Kirk, G.J.D. & Lark, R.M. 2008. Spatial variation of ammonia volatilization from soil and its scale dependent correlation with soil properties. *European Journal of Soil Science*, **59**, 1260–1270.

FAO-Unesco 1974. *Soil Map of the World, 1:5 000 000*, Volume **1**, Legend. Unesco, Paris.

Guo, X.Y., Zuo, Y.B., Wang, B.R., Li, J.M. & Mas, Y.B. 2010. Toxicity and accumulation of copper and nickel in maize plants cropped on calcareous and acidic field soils. *Plant & Soil*, **333**, 365–373.

Hartemink, A.E. & Minasny, B. 2014. Towards digital soil morphometrics. *Geoderma*, **231–231**, 305–317.

Hoosbeek, M.R. & Bryant, R.B. 1992. Towards the quantitative modelling of pedogenesis – a review. *Geoderma*, **55**, 183–210.

Katebe, R., Michalik, B., Phiri, Z. & Nkhuwa, D.C.W. 2008. Status of naturally occurring radionuclides in copper mine wastewater in Zambia. *Naturally Occurring Radioactive Material (NORM V), Proceedings of the Fifth International Symposium on Naturally Occurring Radioactive Material*, Seville, 19–22 March 2007, pp. 409–417. International Atomic Energy Agency, Vienna.

Krige, D.G. 1981. *Lognormal-de Wijsian Geostatistics for Ore Evaluation*. South African Institute of Mining and Metallurgy, Johannesburg.

Lark, R.M. 2011. Spatially nested sampling schemes for spatial variance components: scope for their optimization. *Computers & Geosciences*, **37**, 1633–1641.

Lark, R.M. 2012. Some considerations on aggregate sample supports for soil inventory and monitoring. *European Journal of Soil Science*, **63**, 86–95.

Lottermoser, B.G. 2007. *Mine Wastes: Characterization, Treatment, Environmental Impacts*. Springer, Berlin.

Lovejoy, S. & Schertzer, D. 2007. Scaling and multifractal fields in the solid earth and topography. *Nonlinear Processes in Geophysics*, **14**, 465–502.

McBride, M.B. 1994. *Environmental Chemistry of Soils*. Oxford University Press, New York.

McCullagh, P. & Clifford, D. 2006. Evidence for conformal invariance of crop yields. *Proceedings of the Royal Society A*, **462**, 2119–2143.

Metcalfe, H., Milne, A.E., Webster, R., Lark, R.M., Murdoch, A. & Storkey, J. 2016. Designing a sampling scheme to reveal correlations between weed patches and soil properties at multiple spatial scales. *Weed Research*, **56**, 1–13.

Miesch, A.T. 1975. Variograms and variance components in geochemistry and ore evaluation. *Geological Society of America Memoirs*, **142**, 333–340.

Ministry of Agriculture 1991. *Exploratory Soil Map of Zambia, Scale 1:1.000.000*. Ministry of Agriculture, Lusaka.

National Research Council 1999. *Evaluation of Guidelines for Exposures to Technologically Enhanced Naturally Occurring Radioactive Materials*. The National Academies Press, Washington, DC.

Oliver, M.A. & Webster, R. 1987. The elucidation of soil pattern in the Wyre forest of the West-Midlands, England. II. Spatial-distribution. *Journal of Soil Science*, **38**, 293–307.

Pachepsky, Y. & Hill, R.L. 2017. Scale and scaling in soils. *Geoderma*, **287**, 4–30.

Papritz, A., Dümig, A., Zimmermann, C., Gerke, H.H., Felderer, B., Kögel-Knabner, I. *et al.* 2011. Uncertainty of variance component estimates in nested sampling: a case study on the field-scale spatial variability of a restored soil. *European Journal of Soil Science*, **62**, 479–495.

Percival, D.B. & Walden, A.T. 2000. *Wavelet Methods for Time Series Analysis*. Cambridge University Press, Cambridge.

Petruzzelli, G., Guidi, G. & Lubrano, L. 1978. Organic matter as an influencing factor on copper and cadmium adsorption by soils. *Water, Air, & Soil Pollution*, **9**, 263–269.

Pinheiro, J.C. & Bates, D.M. 2000. *Mixed Effects Models in S and S-Plus*. Springer, New York.

R Core Team 2014. *R: A Language and Environment for Statistical Computing*. R Foundation for Statistical Computing, Vienna. [WWW document]. URL http://www.R-project.org/ [accessed on 01 April 2017].

Stram, D.O. & Lee, J.W. 1994. Variance components testing in the longitudinal mixed effects setting. *Biometrics*, **50**, 1171–1177.

Temminghoff, E.J.M., Van der Zee, S.E.A.T.M. & De Haan, F.A.M. 1998. Effects of dissolved organic matter on the mobility of copper in a contaminated sandy soil. *European Journal of Soil Science*, **49**, 616–128.

Vogel, H.-J. & Roth, K. 2003. Moving through scales of flow and transport in soil. *Journal of Hydrology*, **272**, 95–106.

Wagenet, R.J. 1998. Scale issues in agroecological research chains. *Nutrient Cycling in Agroecosystems*, **50**, 23–34.

Webster, R. 1965. A catena of soils on the Northern Rhodesia plateau. *Journal of Soil Science*, **16**, 31–43.

Webster, R. 2000. Is soil variation random? *Geoderma*, **97**, 149–163.

Webster, R. & Boag, B. 1992. A geostatistical analysis of cyst nematodes in soil. *Journal of Soil Science*, **43**, 583–595.

Webster, R. & Oliver, M.A. 1990. *Statistical Methods in Soil and Land Resource Survey*. Oxford University Press, Oxford.

Webster, R., Welham, S.J., Potts, J.M. & Oliver, M.A. 2006. Estimating the spatial scales of regionalized variables by nested sampling, hierarchical analysis of variance and residual maximum likelihood. *Computers & Geosciences*, **32**, 1320–1333.

Weissenstein, K. & Sinkala, T. 2011. Soil pollution with heavy metals in mine environments, impact areas of mine dumps particularly of gold and copper mining industries in southern Africa. *Arid Ecosystems*, **1**, 53–58.

Wilson, A.T., Ballantyne, A.O., Brockington, N.R. & Rees, A.M. 1956. *Report of a Soil and Land-Use Survey, Copperbelt, Northern Rhodesia*. Department of Agriculture, Lusaka.

Youden, W.J. & Mehlich, A. 1937. Selection of efficient methods for soil sampling. *Contributions of the Boyce Thompson Institute for Plant Research*, **9**, 59–70.